N-Bonded Monosilanols: Synthesis and Characterization of ArN($SiMe_3$)$SiMe_2Cl$ and ArN($SiMe_3$)$SiMe_2OH$ (Ar = C_6H_5, 2,6-$Me_2C_6H_3$, 2,6-*i*$Pr_2C_6H_3$)

Vadapalli Chandrasekhar,*[a] Ramamoorthy Boomishankar,[a] Ramachandran Azhakar,[a] Kandasamy Gopal,[a] Alexander Steiner,[b] and Stefano Zacchini[b]

Keywords: Monosilanols / *N*-Bonded silanols / Hydrogen bonding / Aminosilanols

By the use of aniline and the sterically hindered aromatic primary amines, 2,6-$Me_2C_6H_3NH_2$ and 2,6-*i*$Pr_2C_6H_3NH_2$, *N*-bonded monochlorosilanes, ArN($SiMe_3$)$SiMe_2Cl$ [Ar = C_6H_5 (**1a**), Ar = 2,6-$Me_2C_6H_3$ (**1b**) and Ar = 2,6-*i*$Pr_2C_6H_3$ (**1c**)] have been prepared by a sequential deprotonation at the nitrogen followed by reaction with silyl chlorides. Hydrolysis of the *N*-bonded monochlorosilanes afforded the *N*-bonded monosilanols ArN($SiMe_3$)$SiMe_2OH$ [Ar = C_6H_5 (**2a**), Ar = 2,6-$Me_2C_6H_3$ (**2b**) and Ar = 2,6-*i*$Pr_2C_6H_3$ (**2c**)]. The X-ray crystal structure of **1c** reveals a positional disorder of the Cl and CH_3 substituents on silicon. The X-ray crystal structure of **2c** shows that it is involved in an intermolecular O–H···O hydrogen bonding in the solid state to afford a dimeric structure containing the O_2H_2 ring.
(© Wiley-VCH Verlag GmbH & Co. KGaA, 69451 Weinheim, Germany, 2005)

Introduction

Silanols as compounds containing Si–OH units are attracting considerable interest in recent years because of various reasons. They are excellent precursors for the synthesis of main group and transition metal siloxanes containing the Si–O–M bonds.[1,2] Thus, the reaction of appropriate silanols with suitable metal substrates such as metal halide, hydride, -alkyl, amide or alkoxide leads to the formation of acyclic, cyclic or cage metallasiloxanes.[1,3,4] Often the nature of the synthesized metallasiloxane depends on the type of silanol chosen.[3] A second reason of interest in silanols is their utility to serve as models for silica surfaces particularly in the context of silica-supported transition metal catalysts.[5] More recently, there has also been considerable interest in silanols in organic synthesis.[6a] For example, silanols have been found to be excellent substrates for palladium-catalyzed (and fluoride-, cesium carbonate- or silver oxide-activated) cross-coupling reactions.[6b–6d] The utility of silanols in Mizoroki–Heck-type of coupling reactions has also been demonstrated.[6e] Finally silanols are also gaining importance as bioisosteres with specific interest as transition-state analogues for metalloproteases, aspartic proteases as well as HIV proteases.[7]

Among the various types of silanols that have been reported, monosilanols of the type R_3SiOH, $R_2R'SiOH$ and $RR'R''SiOH$ are the simplest examples as these contain only one Si–OH group per molecule.[8] Although several types of monosilanols are known,[8] there are *none* which contain Si–N bonds. One of the possible reasons for this lacuna is probably the high sensitivity of the Si–N bond towards hydrolysis.[9] On the other hand about 70 to 80% of all silanols are actually synthesized by a hydrolysis reaction of an appropriate Si–X bond (X = F, Cl, Br, I or OR).[8] Recent pioneering efforts of Roesky and coworkers,[10] and our interest in ***N***-bonded silanols[11] has prompted us to assemble *N*-bonded monosilanols. Accordingly, herein, we report the synthesis and spectroscopic characterization of ArN($SiMe_3$)$SiMe_2Cl$ [Ar = C_6H_5 (**1a**), 2,6-$Me_2C_6H_3$ (**1b**), 2,6-*i*$Pr_2C_6H_3$ (**1c**)] and ArN($SiMe_3$)-$SiMe_2OH$ [Ar = C_6H_5 (**2a**), 2,6-$Me_2C_6H_3$ (**2b**), 2,6-*i*$Pr_2C_6H_3$ (**2c**)]. We also report the X-ray structural characterization of **1c** and **2c**.

Results and Discussion

Synthesis and Spectra: Sterically unencumbered as well as hindered aromatic amines (aniline, 2,6-dimethylaniline, 2,6-diisopropylaniline) were used as the starting materials. Sequential deprotonation at nitrogen followed by reaction with silyl halides afforded the *N*-bonded silyl chlorides **1a**, **1b** in excellent yields as distillable oils or as a solid (**1c**) (Scheme 1). In contrast to the situation with corresponding *N*-bonded silicon dichlorides and trichlorides **1b** and **1c** are quite stable to ambient moisture. The compound **1a**, however, is sensitive to ambient moisture and undergoes hydrolysis to the silanol **2a**.

---

[a] Department of Chemistry, Indian Institute of Technology, Kanpur,
Kanpur 208016, India
Fax: +91-512-2590007-2597436
E-mail: vc@iitk.ac.in
[b] Department of Chemistry, University of Liverpool,
Liverpool, L69 7ZD, U. K.

DOI: 10.1002/ejic.200401013

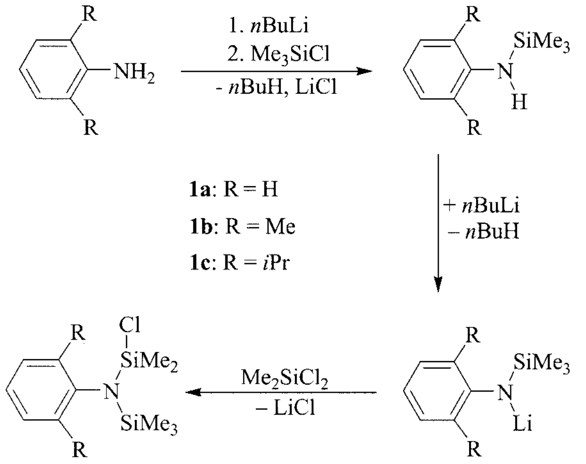

1a: R = H
1b: R = Me
1c: R = iPr

Scheme 1.

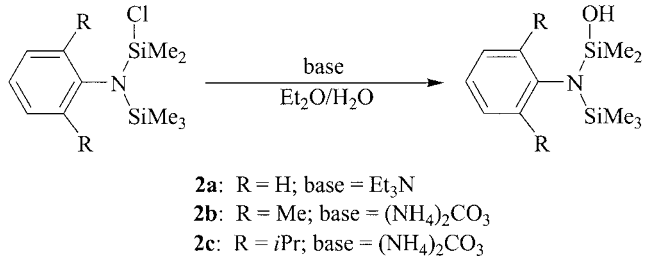

2a: R = H; base = Et$_3$N
2b: R = Me; base = (NH$_4$)$_2$CO$_3$
2c: R = iPr; base = (NH$_4$)$_2$CO$_3$

Scheme 2.

Hydrolysis of **1a**, **1b** and **1c** afford the corresponding monosilanols **2a**, **2b** and **2c** (Scheme 2). While hydrolysis of **1a** is effected by the use of triethylamine as the hydrogen chloride scavenger, hydrolysis of **1b** and **1c** require ammonium carbonate. It is important to note that the use of aniline, which is very effective as a mild base for the hydrolysis of *N*-bonded silicon dichlorides and trichlorides, does not result in clean hydrolysis of **1a**, **1b** or **1c**. Although the silanols **2a** and **2b** are isolated as oils, **2c**, which contains the sterically hindered aromatic amine substituent, is a solid. While **2a**, **2b** and **2c** are rare examples of *N*-bonded monosilanols, **2a** represents the first example of *any* silanol (monosilanol, silanediol or silanetriol) where the sterically *unencumbered* aniline is the substituent on silicon.

The new *N*-bonded silyl chlorides and silanols are extremely lipophilic and are soluble in a wide range of organic solvents. The compounds **1a**–**c** and **2a**–**c** have been characterized by mass spectroscopy, elemental analysis, IR spectroscopy and multi-nuclear NMR spectroscopy. The silyl chlorides and the monosilanols show prominent parent ion peaks in their FAB mass spectra. The ^{1}H NMR spectra of these compounds are consistent with their structures. The ^{29}Si {^{1}H} NMR spectra of the silyl chlorides are characterized by chemical shifts for the –*Si*Me$_3$ and –*Si*Me$_2$Cl. While the former resonate between δ = 11.9 and 12.6 ppm the latter are seen at a slightly lower frequency between 7.8 and 8.6 ppm, respectively (Table 1). The –*Si*Me$_2$Cl chemical shifts occur at a higher frequency than the corresponding –*Si*MeCl$_2$ (–1.3 and –1.4 ppm)[11a] and –*Si*Cl$_3$ (–28.2 and –27.9 ppm).[10a] A movement of the ^{29}Si chemical shift to lower frequency occurs upon conversion of Ar*Si*Me$_2$Cl (**1a**–**1c**) to Ar*Si*Me$_2$OH (**2a**–**2c**). Thus the latter resonate at –1.7 (**2a**), –1.3 (**2b**) and –0.8 (**2c**) ppm, respectively. These chemical shifts are at a higher frequency in comparison to the corresponding silanediols (–29.4 and –29.6 ppm)[11a] and silanetriols (–66.2 and –65.3 ppm).[10a]

The IR spectra of the silanediols **2a** and **2b** in the solid sate in KBr pellets show broad bands at 3350 and 3416 cm^{-1}, respectively. In **2c** in addition to the peak at 3466 cm^{-1} a sharp peak at 3666 cm^{-1} is also observed. The observation of the latter shows that the formation of the KBr pellet disrupts some of the intermolecular hydrogen bonding in **2c** to give rise to free Si–OH.

X-ray Crystal Structures of 1c and 2c: The X-ray crystal structure of **1c** shows a positional disorder; the Cl and CH$_3$ groups attached to silicon are disordered over the same sites (Figure 1). Such a positional disorder occurs because of the similar volumes of the Cl and CH$_3$ groups. This results in the two Si–N distances being the same [1.729(1) Å]. The sum of the bond angles around nitrogen N1 equal 360° reflecting the perfect planarity around nitrogen.

Table 1. ^{29}Si NMR chemical shifts of *N*-bonded silicon chlorides and silanols and related dichlorides, trichlorides, diols and triols.

Compound	δ NSiMe$_3$	δ SiCl	δ SiCl$_2$	δ SiCl$_3$	δ SiOH	δ Si(OH)$_2$	δ Si(OH)$_3$	Ref.
(C$_6$H$_5$)N(SiMe$_3$)(Me$_2$SiCl)	11.9	8.6						this work
(2,6-Me$_2$C$_6$H$_3$)N(SiMe$_3$)(Me$_2$SiCl)	12.3	7.8						this work
(2,6-iPr$_2$C$_6$H$_3$)N(SiMe$_3$)(Me$_2$SiCl)	12.6	7.8						this work
(C$_6$H$_5$)N(SiMe$_3$)(Me$_2$SiOH)	5.0				–1.7			this work
(2,6-Me$_2$C$_6$H$_3$)N(SiMe$_3$)(Me$_2$SiOH)	5.0				–1.3			this work
(2,6-iPr$_2$C$_6$H$_3$)N(SiMe$_3$)(Me$_2$SiOH)	5.0				–0.8			this work
(2,6-Me$_2$C$_6$H$_3$)N(SiMe$_3$)(MeSiCl$_2$)	10.3		–1.3					[11a]
(2,6-iPr$_2$C$_6$H$_3$)N(SiMe$_3$)(MeSiCl$_2$)	10.4		–1.4					[11a]
(2,6-Me$_2$C$_6$H$_3$)N(SiMe$_3$)(MeSi(OH)$_2$)	5.7					–29.4		[11a]
(2,6-iPr$_2$C$_6$H$_3$)N(SiMe$_3$)(MeSi(OH)$_2$)	5.6					–29.6		[11a]
(2,6-Me$_2$C$_6$H$_3$)N(SiMe$_3$)SiCl$_3$	12.5			–28.2				[10a]
(2-Me-6-iPr$_2$C$_6$H$_3$)N(SiMe$_3$)SiCl$_3$	12.2			–27.9				[10a]
(2,6-Me$_2$C$_6$H$_3$)N(SiMe$_3$)Si(OH)$_3$	7.7						–66.2	[10a]
(2-Me-6-iPr$_2$C$_6$H$_3$)N(SiMe$_3$)Si(OH)$_3$	7.5						–65.3	[10a]

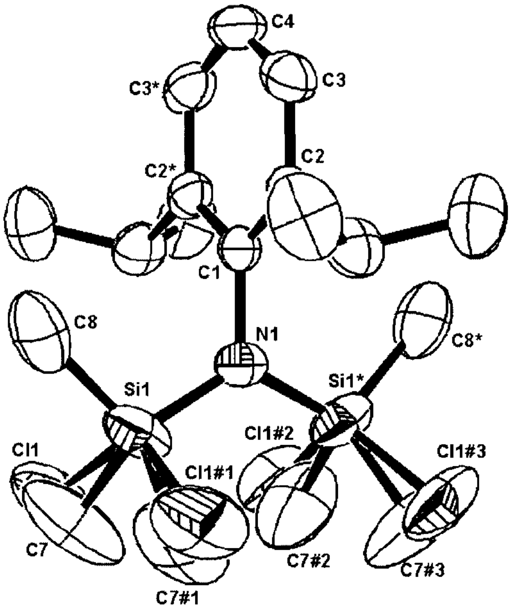

Figure 1. ORTEP diagram of **1c** shown at the 50% probability level. All the hydrogen atoms are omitted for clarity.

The ORTEP diagram of **2c** is shown in Figure 2. Unlike in **1c** two types of Si–N bond lengths are seen viz., Si1–N1, 1.731(1) and Si2–N1, 1.759(1) Å. The longer bond distance is associated with the silicon bearing less electronegative substituents while the shorter distance is associated with *N-Si*Me$_2$OH. The shorter Si1–N1 distance is however, longer than the corresponding distance of 1.7140(18) Å observed in 2,4,6-Me$_3$C$_6$H$_2$–N(SiMe$_3$)SiMe(OH)$_2$. The Si1–O1 distance of 1.648(2) Å is consistent with the trends found in other silanols. This value is shorter than the sum of the covalent radii of silicon and oxygen (1.74 Å). The geometry around nitrogen (N1) is perfectly planar with all the angles around it totaling to 360°.

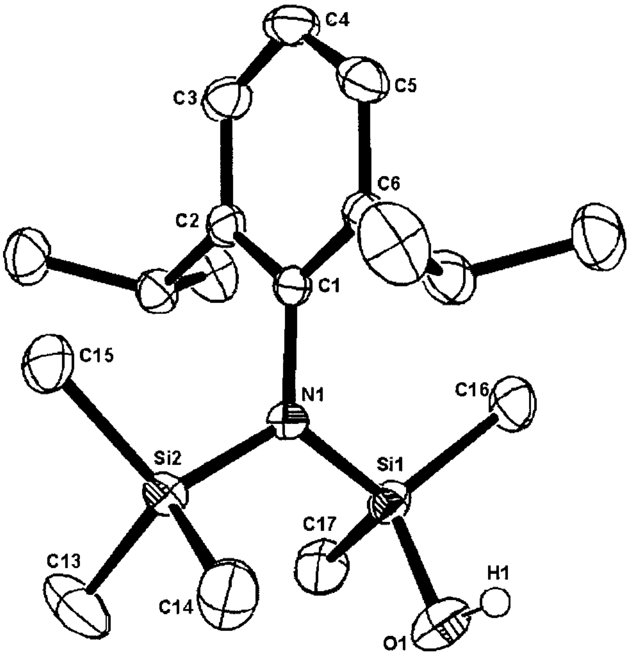

Figure 2. ORTEP diagram of **2c** shown at the 50% probability level. All the hydrogen atoms have been omitted except those of the hydroxy group.

Intermolecular hydrogen bonding in monosilanols can give rise to different types of arrangements in the solid state, such as a linear dimer,[14a] cyclic dimer,[14b] tetramer,[14c] zigzag polymer[14d] etc. The *N*-bonded monosilanol **2c** shows a cyclic dimer formation (Figure 3) which is quite rare and has been shown before only by the monosilanols containing direct Si–M bonds viz., [(η^5-Cp*)Ru(CO)$_2$]Si(*o*-Tolyl)$_2$-(OH)[14b] and [(η^5-Cp)Fe(CO)$_2$]$_2$Si(H)(OH).[14e] In the solid state two molecules of **2c** interact with each other and form a planar four-membered O$_2$H$_2$ ring. The intermolecular H···O distance is 2.057(1) Å, while the O···O contact is 2.857(2) Å. The O–H···O angle is 158.94(9)°. It is of interest to compare these parameters with those observed earlier. Thus for {(η^5-Cp*)Ru(CO)$_2$}Si(*o*-Tolyl)$_2$(OH) the hydrogen bonding parameters are H···O, 2.172(27) Å. O···O, 2.809(32) Å and O–H···O 134.57(2)°. For {(η^5-Cp)Fe-(CO)$_2$}$_2$Si(H)(OH) these values are 2.197 and 2.991 Å and 157.95°.[14b] Thus, the observed hydrogen bonding parame-

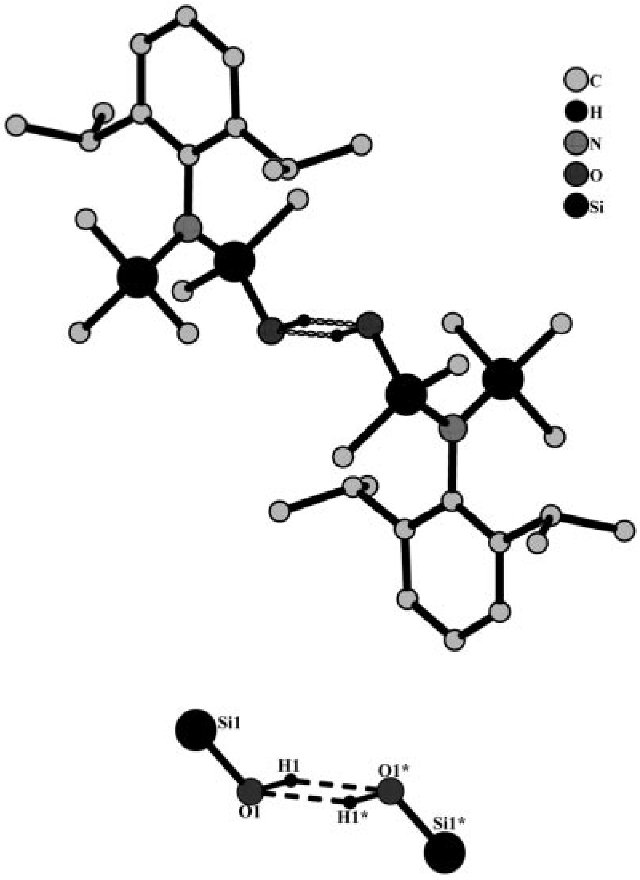

Figure 3. (Top). Formation of a cyclic dimer due to intermolecular hydrogen bonding between two silanol molecules. (Bottom). A perfectly planar arrangement of the four-membered O$_2$H$_2$ ring. The metric parameters are: O1–H1, 0.840(1) Å; H1···O1*, 2.057(1) Å; O···O*, 2.857(2) Å; O–H···O*, 158.94(9)°; symmetry, $1 - x$, $1 - y$, $2 - z$.

ters in **2c** are quite reasonable and indicate the presence of a strong intermolecular hydrogen bonding.

Conclusions

In conclusion we have demonstrated the synthesis of the new examples of *N*-bonded monosilanols. These syntheses were accomplished starting from aromatic amines. A highlight of the synthesis was that for the first time unsubstituted aniline could be utilized to afford an *N*-bonded silanol. X-ray crystal structure of the monosilanol **2c** showed the presence of a hydrogen bonded dimer in the solid-state. All the silanols are extremely lipophilic and air-stable. The utility of these *N*-bonded monosilanols in the assembly of metallasiloxanes is under investigation.

Experimental Section

General Remarks: All manipulations and reactions were carried out under dry nitrogen by employing standard Schlenk techniques. Solvents were dried with sodium benzophenone ketyl and were collected from the still at the time of reaction. 2,6-Dimethylaniline and 2,6-diisopropylaniline (Fluka) were distilled under reduced pressure before use. Chlorotrimethylsilane, dichlorodimethylsilane (Fluka) and *n*-butyllithium (2.5 m solution in hexane) (Aldrich) were used as such without any further purification. Aniline (Spectrochem, India) was stored over CaH$_2$ and distilled before use. Infrared spectra were recorded in dichloromethane solution as well as neat liquid or as KBr pellets with a FT-IR Bruker-Vector Model. Elemental Analyses were performed with Thermoquest CE instruments CHNS–O, EA/110 model. FAB mass spectra were recorded with a JEOL-SX 102/DA-6000 mass spectrometer/data system using argon/xenon (6 kV, 10 mA) as the FAB gas. The accelerating voltage was 10 kV, and the spectra were recorded at room temperature. EI mass spectra were obtained with a JEOL-d-300 spectrometer. The ^{29}Si {^{1}H}, and ^{1}H NMR spectra were recorded in CDCl$_3$ solutions with a JEOL JNM LAMBDA 400 model spectrometer. Chemical shifts are reported with respect to TMS.

Synthesis: The *N*-bonded monochlorosilanes **1a**, **1b** and **1c** and the corresponding silanols **2a**, **2b**, and **2c** were synthesized by adopting the following general synthetic procedure. The ^{29}Si NMR spectroscopic data for these compounds along with some of the other related compounds are listed in Table 1.

Synthesis of the *N*-Bonded Monochlorosilanes, ArN(SiMe$_3$)SiMe$_2$Cl (1a–1c) [Ar = C$_6$H$_5$ (1a), R = 2,6-Me$_2$C$_6$H$_3$ (1b), 2,6-*i*Pr$_2$C$_6$H$_3$ (1c)]: *n*-Butyllithium (75 mmol) was added at a constant rate to a solution of RNH$_2$ (75 mmol) in diethyl ether (60 mL) at –78 °C. The reaction mixture was stirred at this temperature for 4 h and then brought to ambient temperature. It was then treated with a solution of Me$_3$SiCl (75 mmol) in diethyl ether (40 mL) at –78 °C and allowed to come to room temperature. The precipitated LiCl was filtered and the filtrate was treated with *n*BuLi (75 mmol) at room temperature. After heating under reflux for 4 h the solution was transferred to a pressure-equalizing funnel and added drop wise to a solution of Me$_2$SiCl$_2$ (75 mmol) in diethyl ether (40 mL) and stirred overnight. The precipitated LiCl was filtered and the volatiles from the filtrate were removed in vacuo to give a yellow viscous oily product. Subsequent vacuum distillation afforded the pure silicon chlorides **1a** and **1b** as colorless oily liquids. Compound **1c** was isolated as a solid.

Synthesis of *N*-Bonded Monosilanols. Synthesis of C$_6$H$_5$N(SiMe$_3$)-SiMe$_2$OH (2a): A solution of C$_6$H$_5$N(SiMe$_3$)SiMe$_2$Cl (**1a**) (12.2 mmol) in Et$_2$O (50 mL) was added to a well-stirred mixture of Et$_2$O (50 mL), water (12.2 mmol) and triethylamine (12.2 mmol) at 0 °C over a period of 1 h. It was then allowed to come to room temperature and stirred for 30 h. The precipitated triethylamine hydrochloride was filtered. Removal of solvent from the filtrate in vacuo afforded **2a** as a colorless oil.

Synthesis of 2b and 2c: RN(SiMe$_3$)SiMe$_2$Cl (**1b** and **1c**) (12.0 mmol) in diethyl ether (20 mL) was added dropwise through a pressure-equalizing funnel for about 30 min into a rapidly stirred two-phase system consisting of 20 mL of water, 20 mL of diethyl ether and 1.0 g (10.0 mmol) of freshly titrated ammonium carbonate and sodium chloride (7.0 g). The solution was then stirred for another 2 h. The ether layer was separated and the aqueous layer was extracted twice with ether. The combined ether fractions were dried to get crude **2b** and **2c**. The compound **2b** was purified on a neutral alumina column using *n*-hexane/ethyl acetate (90:10) as the eluent to get a pale yellow oil. Compound **2c** was purified by repeated recrystallization from a solution of *n*-hexane.

Characterization Data for Compounds 1a–c and 2a–c

[C$_6$H$_5$N(SiMe$_3$)SiMe$_2$Cl] (1a): Yield 14.7 g (75.9%). B.p. 135 °C/0.08 Torr. C$_{11}$H$_{20}$ClNSi$_2$: calcd. C 51.23, H 7.82, N 5.43; found C 51.04, H 7.31, N 5.31. Mass spectrum (EI): *m*/*z* = 258 (41.5) [M]$^+$, (1 Cl isotope pattern). ^{1}H NMR (400 MHz, CDCl$_3$): δ = 6.85–7.08 (m, 5 H, aromatic), 0.22 [s, 6 H, Si(CH_3)$_2$Cl], 0.00 [s, 9 H, Si(CH_3)] ppm.

[2,6-Me$_2$C$_6$H$_3$N(SiMe$_3$)SiMe$_2$Cl] (1b): Yield 15.2 g (75.9%). B.p. 143 °C/0.08 Torr. C$_{13}$H$_{24}$ClNSi$_2$: calcd. C 54.60, H 8.46, N 4.90; found C 54.22, H 8.17, N 4.55. Mass spectrum (FAB): *m*/*z* = 286 (29) [M$^+$] (1 Cl isotope pattern). ^{1}H NMR (400 MHz, CDCl$_3$): δ = 6.76–6.84 (m, 3 H, aromatic), 2.13 (s, 6 H, C–CH_3), 0.20 [s, 6 H, Si(CH_3)$_2$Cl], 0.00 [s, 9 H, Si(CH_3)] ppm.

[2,6-*i*Pr$_2$C$_6$H$_3$N(SiMe$_3$)SiMe$_2$Cl] (1c): Yield 16.9 g (66.0%). M.p. 108 °C. C$_{17}$H$_{32}$ClNSi$_2$: calcd. C 59.69, H 9.43, N 4.09; found C 59.59, H 8.55, N 3.89. Mass spectrum (FAB): *m*/*z* = 342 (45) [M$^+$] (1 Cl isotope pattern). ^{1}H NMR (400 MHz, CDCl$_3$): δ = 6.89–6.96 (m, 3 H, aromatic); 3.30 [septet, ^3J(H,H) = 6.8 Hz 2 H, HC-(CH$_3$)$_2$], 1.03 [d, ^3J(H,H) = 6.84 Hz, 6 H, CH–CH_3], 1.04 [d, ^3J(H,H) = 6.8 Hz, 6 H, CH–CH_3], 0.21 [s, 6 H, Si(CH_3)$_2$Cl], 0.00 [s, 9 H, Si(CH_3)] ppm.

[C$_6$H$_5$N(SiMe$_3$)SiMe$_2$OH] (2a): Yield 2.7 g (82.1%). C$_{11}$H$_{21}$NOSi$_2$: calcd. C 55.17, H 8.84, N 5.85; found C 54.64, H 8.43, N 5.42. ^{1}H NMR (400 MHz, CDCl$_3$): δ = 6.81–7.14 (m, 5 H, aromatic), 0.01 [s, 6 H, OSi(CH_3)], 0.00 [s, 9 H, Si(CH_3)] ppm.

[2,6-Me$_2$C$_6$H$_3$N(SiMe$_3$)SiMe$_2$OH] (2b): Yield 2.6 g (76.0%). C$_{13}$H$_{25}$NOSi$_2$: calcd. C 58.37, H 9.42, N 5.24; found C 58.21, H 9.08, N 5.11. Mass spectrum (FAB): *m*/*z* = 267 (47) [M]$^+$. ^{1}H NMR (400 MHz, CDCl$_3$): δ = 6.75–6.89 (m, 3 H, aromatic), 2.16 (s, 6 H, C–CH_3), 0.02 [s, 6 H, OSi(CH_3)$_2$], 0.00 [s, 9 H, Si(CH_3)] ppm.

[2,6-*i*Pr$_2$C$_6$H$_3$N(SiMe$_3$)SiMe$_2$OH] (2c): Yield 3.5 g (87.0%). M.p. 108 °C. C$_{17}$H$_{33}$NOSi$_2$: calcd. C 63.09, H 10.28, N 4.33; found C 63.19, H 9.52, N 4.18. Mass spectrum (FAB): *m*/*z* = 323 (70) [M]$^+$. ^{1}H NMR (400 MHz, CDCl$_3$): δ = 6.92–7.13 (m, 3 H, aromatic), 3.35 [m, 2 H, HC(CH$_3$)$_2$, ^3J(H,H) = 6.84 Hz], 1.07 [d, 6 H, CH–CH_3, ^3J(H,H) = 6.84 Hz], 1.08 [d, ^3J(H,H) = 6.56 Hz, 16 H, CH-(CH_3)], 0.04 [s, 6 H, OSi(CH_3)], 0.00 [s, 9 H, Si(CH_3)] ppm.

X-ray Crystallography: Crystals of **1c** and **2c** were grown from a solution of *n*-hexane at –20 °C. Colorless block-like crystals suitable for single-crystal X-ray diffraction were loaded with a Bruker

Table 2. Summary of crystal and structure refinement data for compounds **1c** and **2c**.

Identification code	**1c**	**2c**
Empirical formula	$C_{17}H_{32}ClNSi_2$	$C_{17}H_{33}NOSi_2$
Formula mass	342.07	323.62
Temperature	213(2) K	150(2) K
Wavelength	0.71073 Å	0.71073 Å
Crystal system	orthorhombic	triclinic
Space group	*Cmcm*	$P\bar{1}$
Unit cell dimensions	a = 12.0741(18) Å, α = 90° b = 12.2739(14) Å, β = 90° c = 14.1562(16) Å, γ = 90°	a = 8.4094(5) Å, α = 86.8540(10)° b = 9.6229(6) Å, β = 81.5790(10)° c = 13.0896(8) Å, γ = 71.3230(10)°
Volume	2097.9(5) Å^3	992.61(10) Å^3
Z	4	2
Density (calculated)	1.083 Mg/m^3	1.083 Mg/m^3
Absorption coefficient	0.292 mm^{-1}	0.179 mm^{-1}
F(000)	744	356
Crystal size	0.4 × 0.3 × 0.3 mm^3	0.5 × 0.5 × 0.4 mm^3
Theta range for data collection	2.37 to 24.34°	1.57 to 28.28°
Index ranges	$-14 \le h \le 13$, $-13 \le k \le 13$, $-16 \le l \le 16$	$-10 \le h \le 11$, $-7 \le k \le 12$, $-16 \le l \le 16$
Reflections collected	6518	6325
Independent reflections	915 [R_{int} = 0.0482]	4384 [R_{int} = 0.0410]
Completeness to θ	96.9% (θ = 24.34°)	89.1% (θ = 28.28°)
Absorption correction	none	none
Refinement method	Full-matrix least-squares on F^2	Full-matrix least-squares on F^2
Data/restraints/parameters	915/1/71	4384/0/200
Goodness-of-fit on F^2	1.100	0.986
Final R indices [$I > 2\sigma(I)$]	R_1 = 0.0399, wR_2 = 0.1091	R_1 = 0.0394, wR_2 = 0.1032
R indices (all data)	R_1 = 0.0482, wR_2 = 0.1130	R_1 = 0.0480, wR_2 = 0.1076
Largest diff. peak and hole	0.214 and –0.216 e·Å^{-3}	0.343 and –0.333 e·Å^{-3}

AXS Smart Apex CCD diffractometer. The details pertaining to the data collection and refinement for **1c** and **2c** are given in Table 2. The structures were solved by direct methods using SHELXS-97 and refined by full-matrix least-squares on F^2 using SHELXL-97.[12,13] The hydrogen atom attached to oxygen atom was located from the difference map and its position was refined. All other hydrogen atoms were included in idealized positions, and a riding model was used. Non-hydrogen atoms were refined with anisotropic displacement parameters. Selected bond lengths and bond angles of **1c** and **2c** are given in Table 3 and Table 4.

Table 3. Selected bond lengths [Å] and angles [°] for **1c**.

Bond lengths			
N1–Si1	1.729(1)	Si1–C8	1.857(4)
Si1–Cl1	2.110(5)	Si1–Cl1#3	2.110(5)
Si1–C7	1.853(8)	N1–C1	1.478(4)
Bond angles			
N1–Si1–C8	108.51(12)	N1–Si1–Cl1	107.76(22)
C8–Si1–Cl1	103.51(21)	Cl1–Si1–Cl#1	124.83(16)
N1–Si1–C7	113.42(33)	C8–Si1–C7	113.19(31)
Cl1#1–Si1–C7#1	15.33(27)	Cl1–Si1–C7	109.86(25)
C7–Si1–C7#1	94.74(34)	C1–N1–Si1	117.46(3)
C1–N1–Si1*	117.46(3)	Si1–N1–Si1*	125.08(5)

Symmetry transformations used to generate equivalent atoms #1, #2 and #3: x, y, $-z + {}^3/_2$

Table 4. Selected bond lengths [Å] and angles [°] for **2c**.

Bond lengths			
Si1–N1	1.731(1)	Si1–C16	1.845(2)
Si2–N1	1.759(1)	Si1–C17	1.859(2)
Si1–O1	1.648(2)	N1–C1	1.448(2)
Bond angles			
Si2–N1–Si1	123.60(7)	N1–Si1–O1	107.07(6)
C1–N1–Si1	119.17(9)	C16–Si1–O1	111.56(8)
C1–Si1–Si2	117.22(10)	C17–Si1–O1	103.86(7)

CCDC-229758 and -229759 contain the supplementary crystallographic data for this paper. These data can be obtained free of charge from The Cambridge Crystallographic Data Centre via www.ccdc.cam.ac.uk/data_request/cif.

Acknowledgments

We are thankful to Department of Science and Technology, New Delhi, India for financial support. AS thanks EPSRC (Engineering and Physical Sciences Research Council), U. K. for financial support.

---

[1] a) V. Chandrasekhar, R. Boomishankar, S. Nagendran, *Chem. Rev.* **2004**, *104*, 5847; b) R. Murugavel, A. Voigt, M. G. Walawalkar, H. W. Roesky, *Chem. Rev.* **1996**, *96*, 2205.

[2] a) L. King, A. C. Sullivan, *Coord. Chem. Rev.* **1999**, *189*, 19; b) F. J. Feher, T. A. Budzichowski, *Polyhedron* **1995**, *14*, 3239; c) V. Lorenz, A. Fischer, S. Gießmann, J. W. Gilje, Y. Gun′ko, K. Jacob, F. T. Edelmann, *Coord. Chem. Rev.* **2000**, *206–207*, 321.

[3] a) R. Murugavel, V. Chandrasekhar, H. W. Roesky, *Acc. Chem. Res.* **1996**, *29*, 183; b) R. Murugavel, M. Bhattacharjee, H. W. Roesky, *Appl. Organomet. Chem.* **1999**, *13*, 227; c) G. Anantharaman, H. W. Roesky, J. Magull, *Angew. Chem. Int. Ed.* **2002**, *41*, 1226; d) G. Anantharaman, H. W. Roesky, H.-G. Schmidt, M. Noltemeyer, J. Pinkas, *Inorg. Chem.* **2003**, *42*, 970; e) G. Anantharaman, N. D. Reddy, H. W. Roesky, J. Magull, *Organometallics* **2001**, *20*, 5777.

[4] a) K. L. Fujdala, T. D. Tilley, *Chem. Mater.* **2002**, *14*, 1376; b) M. P. Coles, C. G. Lugmair, K. W. Terry, T. D. Tilley, *Chem.*

Mater. **2000**, *12*, 122; c) C. G. Lugmair, K. L. Fujdala, T. D. Tilley, *Chem. Mater.* **2002**, *14*, 888.

[5] a) R. Duchateau, *Chem. Rev.* **2002**, *102*, 3525; b) H. C. L. Abbenhuis, *Chem. Eur. J.* **2000**, *6*, 25.

[6] a) S. E. Denmark, R. F. Sweis, *Acc. Chem. Res.* **2002**, *35*, 835; b) K. Hirabayashi, J. Kawashima, Y. Nishihara, A. Mori, T. Hiyama, *Org. Lett.* **1999**, *1*, 299; c) K. Hirabayashi, A. Mori, J. Kawashima, M. Suguro, Y. Nishihara, T. Hiyama, *J. Org. Chem.* **2000**, *65*, 5342; d) S. E. Denmark, M. H. Ober, *Org. Lett.* **2003**, *5*, 1357; e) K. Hirabayashi, Y. Nishihara, A. Mori, T. Hiyama, *Tetrahedron Lett.* **1998**, *39*, 7893.

[7] a) S. McN. Sieburth, T. Nittoli, A. M. Mutahi, L. Guo, *Angew. Chem. Int. Ed.* **1998**, *37*, 812; b) M. W. Mutahi, T. Nittoli, L. Guo, S. McN. Sieburth, *J. Am. Chem. Soc.* **2002**, *124*, 7363; c) J. Kim, A.Glekas, S. McN. Sieburth, *Bioorg. Med. Chem. Lett.* **2002**, *12*, 3625; d) C.-A. Chen, S. McN. Sieburth, A. Glekas, G. W. Hewitt, G. L. Trainor, S. Erickson-Viitanen, S. S. Garber, B. Cordova, S. Jeffry, R. M. Klabe, *Chem. Biol.* **2001**, *8*, 1161.

[8] P. D. Lickiss, *Adv. Inorg. Chem.* **1995**, *42*, 147.

[9] R. Murugavel, A. Voigt, V. Chandrasekhar, H. W. Roesky, H.-G. Schmidt, M. Noltemeyer, *Chem. Ber.* **1996**, *129*, 391.

[10] a) R. Murugavel, V. Chandrasekhar, A.Voigt, H. W. Roesky, H.-G. Schmidt, M. Noltemeyer, *Organometallics* **1995**, *14*, 5298; b) N. Winkhofer, A. Voigt, H. Dorn, H. W. Roesky, A. Steiner, D. Stalke, A. Reller, *Angew. Chem. Int. Ed. Engl.* **1994**, *33*, 1352.

[11] a) V. Chandrasekhar, S. Nagendran, R. J. Butcher, *Organometallics* **1999**, *18*, 4488; b) V. Chandrasekhar, S. Nagendran, R. Boomishankar, R. J. Butcher, *Inorg. Chem.* **2001**, *40*, 940.

[12] a) G. M. Sheldrick, SHELXL-97, Program for Crystal Structure Analysis (release 97–2), University of Göttingen, Göttingen, Germany, **1998**.

[13] G. M. Sheldrick, SHELXTL, Version 5.03; Siemens Analytical X-ray Division: Madison, WI, **1994**.

[14] a) M. J. MacLachlan, J. Zheng, K. Thieme, A. J. Lough, I. Manners, C. Mordas, R. LeSuer, W. E. Geiger, L. M. Liable-Sands, A. L. Rheingold, *Polyhedron* **2000**, *19*, 275; b) S. Möller, O. Fey, W. Malisch, W. J. Seelbach, *J. Organomet. Chem.* **1996**, *507*, 239; c) J. Beckmann, K. Jurkschat, M. Schürmann, *J. Organomet. Chem.* **2000**, *602*, 170; d) W. Malisch, M. Hofmann, M. Nieger, W. W. Schöller, A. Sundermann, *Eur. J. Inorg. Chem.* **2002**, 3242; e) W. Malisch, M. Vögler, D. Schumacher, M. Nieger, *Organometallics* **2002**, *21*, 2891.

Received: December 10, 2004